Zero Gravity Test of a 40,000 RPM Flywheel

Alan Brian Palazzolo
Texas A&M University
College Station, Texas

Clinton Johnson*
University of Texas
Austin, Texas

Erwin Thomas and Frank Little
Texas A&M University
College Station, Texas

Jason Preuss*
Barber-Nichols
Denver, Co.

Randall Tucker
Texas A&M
College Station, TX

Andrew Provenza
NASA Glenn
Cleveland, Ohio

ABSTRACT

A zero gravity flight is considered a nearly mandatory prerequisite for flight experiments on the Space Shuttle or International Space Station ISS. NASA Glenn and the Texas A&M Center for Space Power funded an effort to successfully operate a high speed 40,000 rpm flywheel during approximately 100 zero-g parabolic flight trajectories. The total flywheel energy storage system FESS was designed, built and tested at the lead author's Texas A&M laboratory. The magnetic bearings have a fault-tolerant, homopolar design with a load capacity of about 100 lbs in the radial and axial directions. The paper includes design and fabrication details of the flywheel, magnetic suspension and the power, sensing and control systems, and also simulation and flight test results. Other magnetic bearing work presently ongoing in the lead author's lab is also highlighted.

* This work performed as graduate students at Texas A&M University

Dr. Alan Palazzolo, a-palazzolo@tamu.edu, Texas A&M University, Mechanical Engineering, College Station, Tx., 77843-3123, 979-845-5280

(1) INTRODUCTION

Advances in magnetic bearings, power electronics, and composites have allowed flywheel energy storage systems FESS to in some cases surpass electrochemical batteries in terms of achievable energy density, power density, and number of discharge cycles. This is crucial in space applications where weight and longevity is of great concern. Significant research has been performed to optimize and demonstrate the technology can work. This paper documents the authors efforts to demonstrate successful operation of a 40,000 rpm flywheel in a zero g environment. The motivation behind the research was to increase the Technology Readiness Level TRL of the flywheel system, to progress towards flight status. The steps involved were to Develop a design based on rotordynamic simulations including time varying g loads, build and tests the key components of the FESS, test the assembled system in a spin pit at full speed (40 krpm) and finally test the FESS onboard the NASA C-9 zero-g simulator plane. Some of the tests included magnetic bearing load capacity, stiffness and inductance, and journal excursions in the magnetic bearings and bearing currents during power scheduling while at zero and 2 g's.

(2) DESIGN

Figure 1 shows the construction of the FESS including the motor, magnetic bearings, auxiliary (backup) bearings, composite flywheel and shaft.

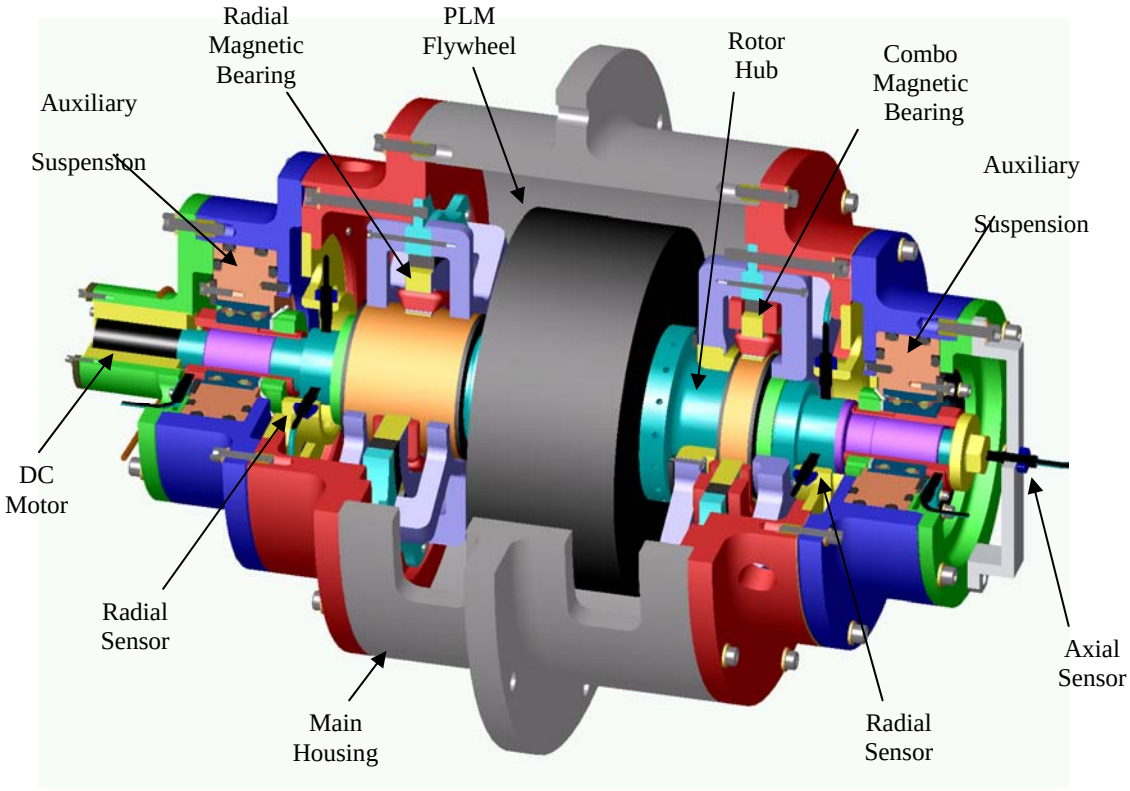

Figure 1 FESS Solid Model

Dr. Alan Palazzolo, a-palazzolo@tamu.edu, Texas A&M University, Mechanical Engineering, College Station, Tx., 77843-3123, 979-845-5280

The shaft material is titanium and the motor is a permanent magnet, brushless DC motor. The rotor and stator lamination stack material and magnetic return paths (back iron) is Hiperco 50A, which is a cobalt – iron alloy. Hard mounted ball bearings are positioned to provide backup support in case of a magnetic bearing failure. A radial magnetic bearing provides pure radial support and a combination magnetic bearing provides axial and radial support. Both are permanent magnet bias, homopolar magnetic bearings with redundant, fail-safe capability [1]. The wheel is composed of concentric carbon fiber composite rings. All of the rings have an interference fit between them and are pressed together with a thin layer of epoxy. The FESS's composite wheel has a 7.35" OD x 3.5" ID x 3" length and stores approximately 50 watt hrs of kinetic energy at 40,000 rpm. The flywheel spin axis is pointed in the wing to wing direction. The weight of the rotating assembly is approximately 20 lbs. The catcher bearing radial clearance was approximately 0.004" and the axial and magnetic bearing radial gaps were all approximately 0.020".

Figure 2 shows a wiring diagram for the radial, fault tolerant, PM biased, homopolar magnetic bearing [1,2]. The CDM box contains circuitry to convert the two transverse X-Z controller outputs into inputs for the 6 PWM servo power amplifiers that supply current to the radial control coils and operate at 80V A decoupling choke is employed to diagonalize the inductance matrix and eliminate a singularity as explained in [2, 3].

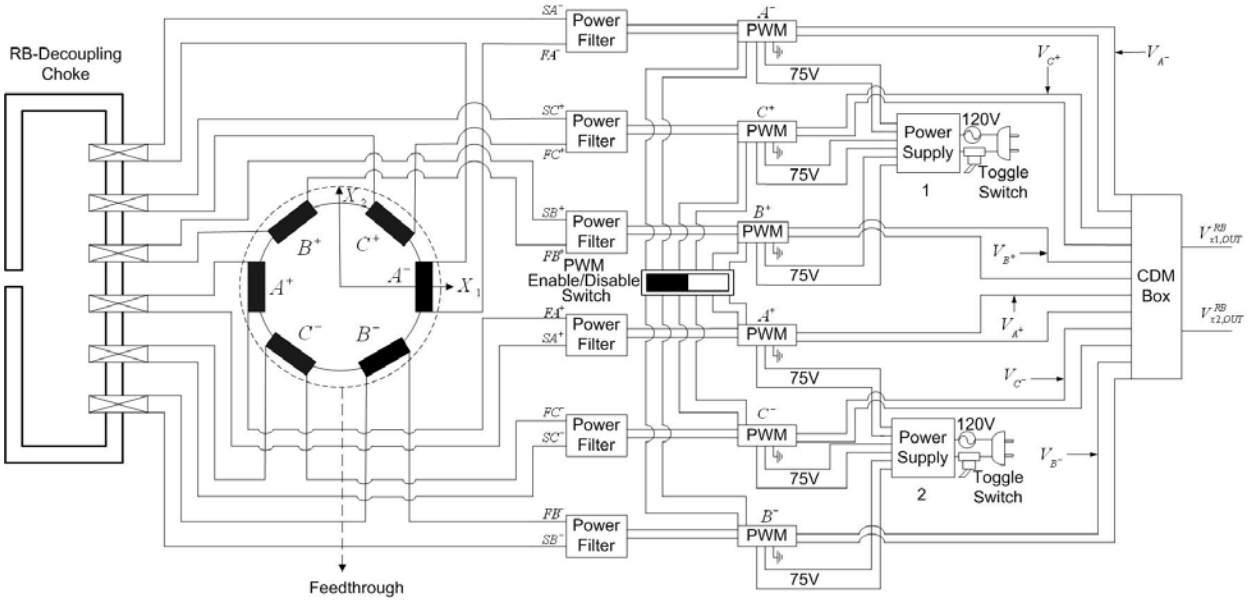

Figure 2 Wiring Diagram for Fault Tolerant Homopolar Magnetic Bearing

The fault tolerant capability was demonstrated on ground tests of another flywheel at NASA Glenn but was tested on the zero-g flywheel. Simulation studies also confirmed the fault tolerance effectiveness

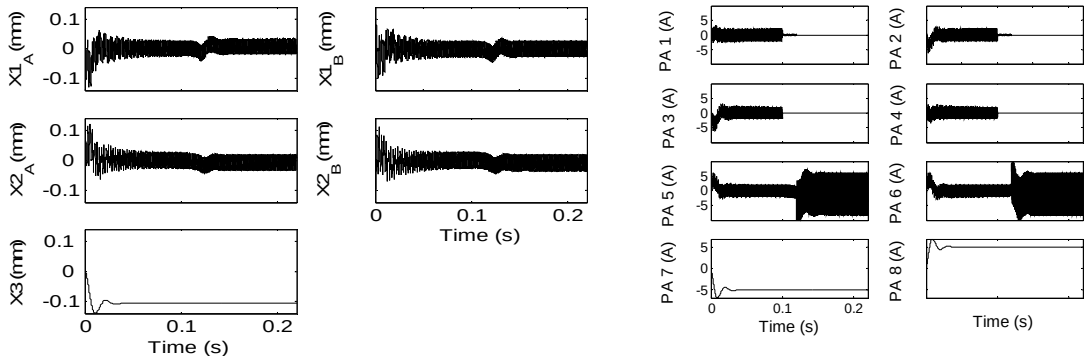

Figure 3 Simulation for Open Circuit on 4 of 6 Poles on Combination Bearing and Continued Levitation

Dr. Alan Palazzolo, a-palazzolo@tamu.edu, Texas A&M University, Mechanical Engineering, College Station, Tx., 77843-3123, 979-845-5280

as shown in Figure 3, where currents in 4 of 6 poles are open circuited, and levitation continues. The control law employed for the magnetic suspension was a direct SISO approach with PD, lead – lag and notch stages. The system was only weakly gyroscopic due to the small diameter of the wheel and low IP/IT ration (approximately 1/3). Ref. [4] will provide an effective approach for MIMO control of highly gyroscopic flywheel systems.

(3) MODELING / SIMULATION

Models were constructed and simulations performed on critical components and for the entire electromechanical system. For example Figure 4 shows the 3D magnetic field model made for the radial magnetic bearing. The model included the nonlinear (saturation) characteristics of the material.

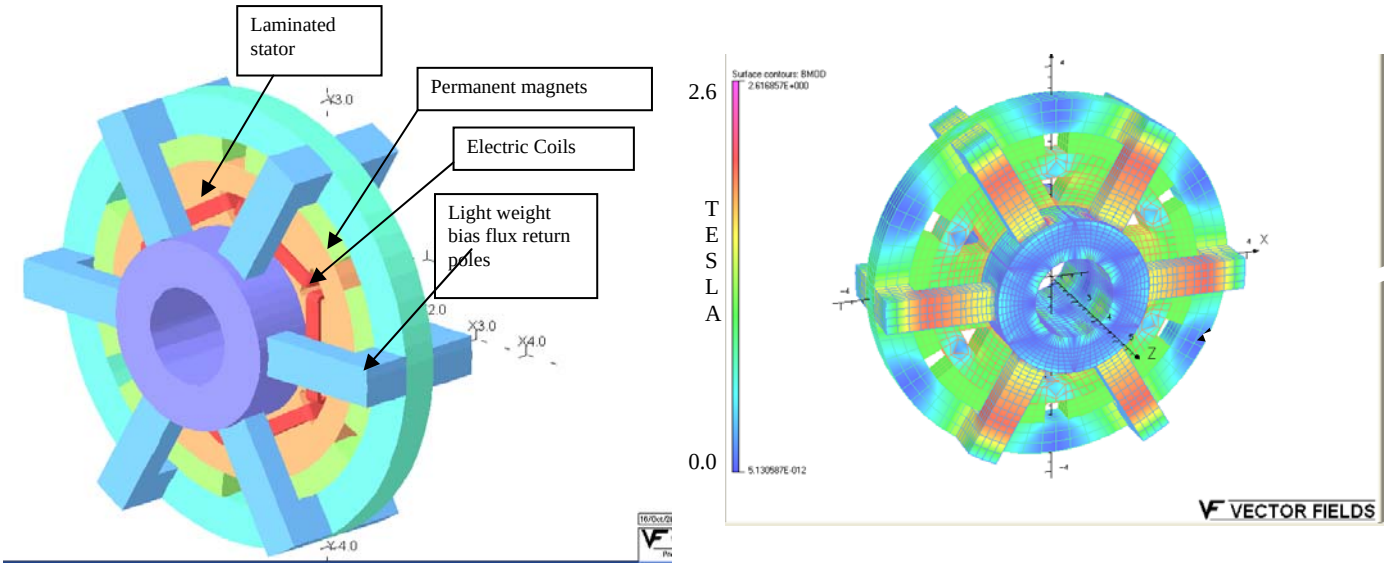

Figure 4 3D Finite Element Based Magnetic Field Model of the Radial, Homopolar Magnetic Bearing

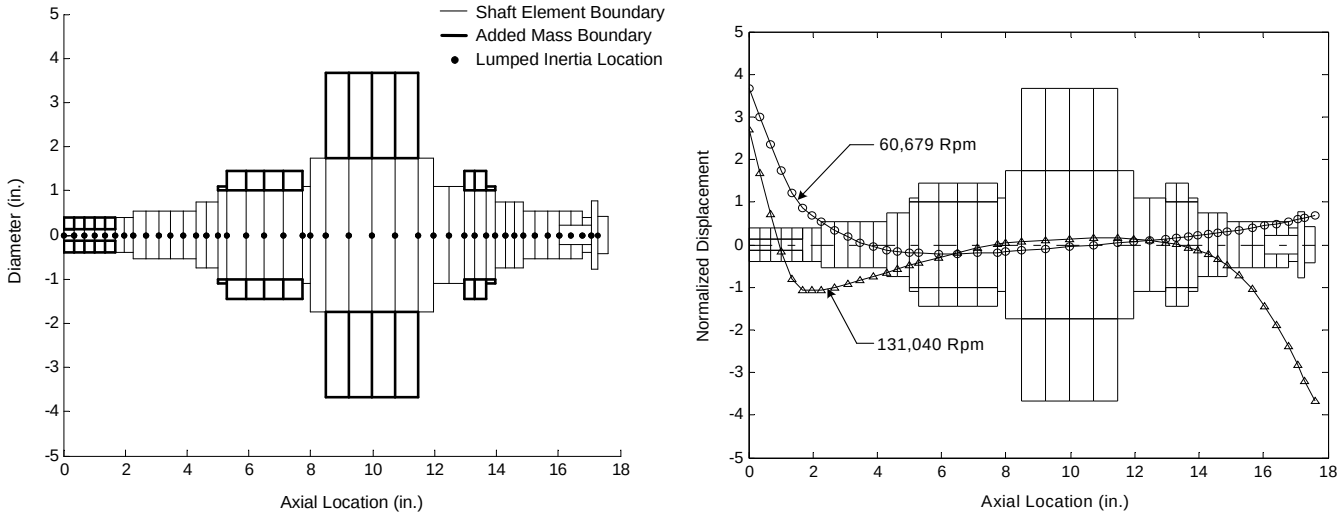

Figure 5 Finite Element Beam Model of Rotating Assembly and Free-Free Modes

Dr. Alan Palazzolo, a-palazzolo@tamu.edu, Texas A&M University, Mechanical Engineering, College Station, Tx., 77843-3123, 979-845-5280

This magnetic field model was employed to minimize weight and provide estimates of load capacity, current and position stiffness, inductance and eddy current drag loss. A similar study was performed for the combination bearing. The flux contour plot corresponds to inclusion of permanent magnet effects only so the flux density exhibits a uniform cyclic symmetry. Figure 5 shows the finite element model of the shaft , which is coupled with component models of the magnetic suspension's controller, magnetic bearings, servo power amplifiers, sensors and actuators to form a complete system electromechanical dynamics simulation model. This model was employed to predict closed loop stability and mode shapes along with response to imbalance, runout and maneuver "g" loading as shown in figure 6

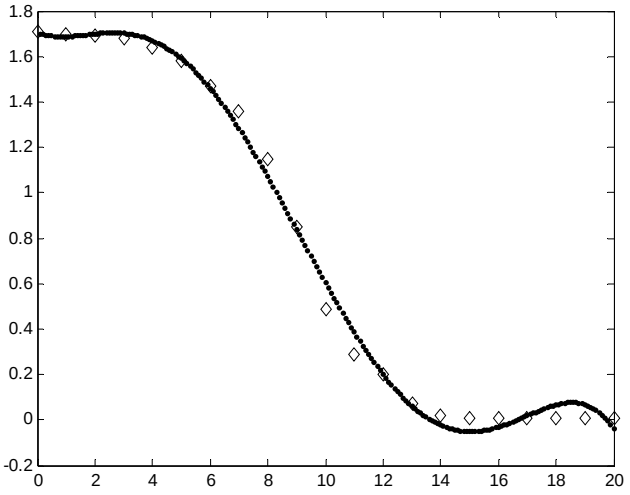

Figure 6 Typical Maneuver "g" Loading Vs. Time(sec.)

Figure 7 and 8 show the predicted journal deflections in the magnetic bearing and the currents corresponding to the "g" loading direction.

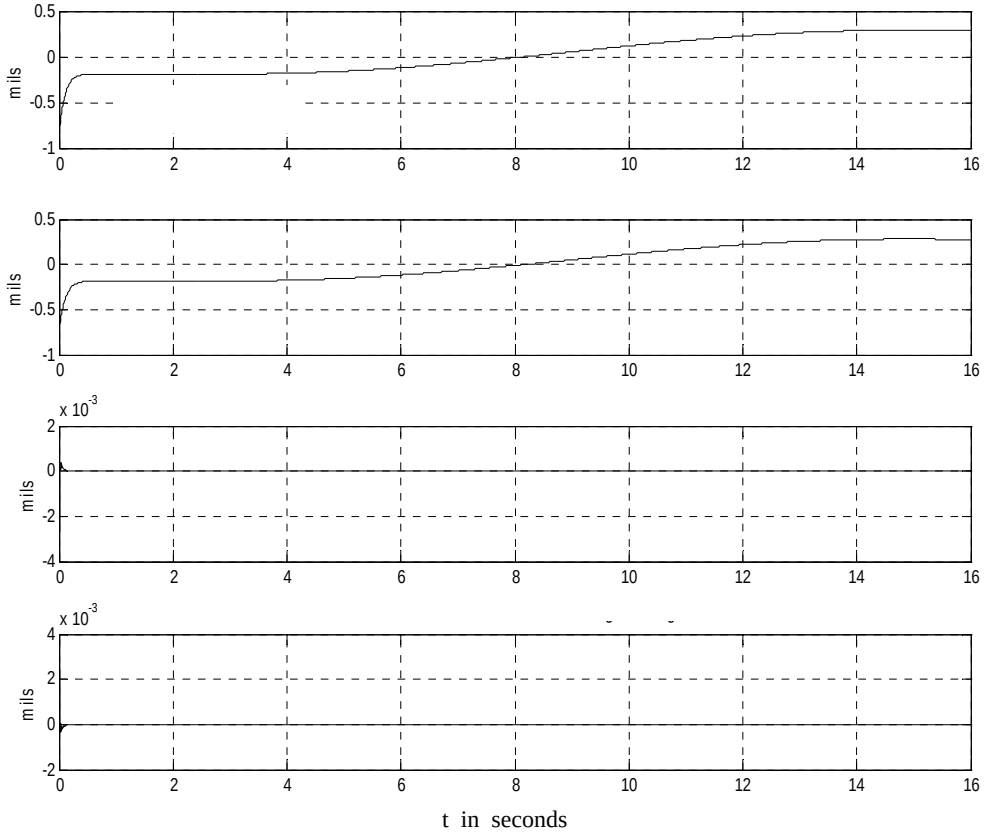

Figure 7 Predicted Journal Deflections Referenced to 1g Static Deflection

Dr. Alan Palazzolo, a-palazzolo@tamu.edu, Texas A&M University, Mechanical Engineering, College Station, Tx., 77843-3123, 979-845-5280

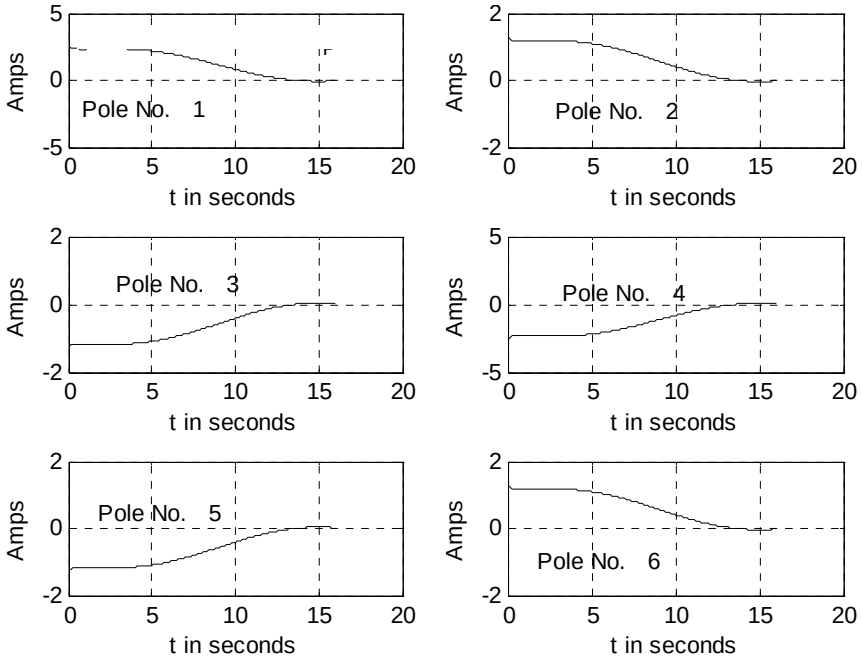

Figure 8 Predicted Radial Bearing Currents Due to "g" Loading

Figure 9 shows the Campbell diagram for the cylindrical and conical modes. The speed dependence of the gyroscopic conical modes is clearly present.

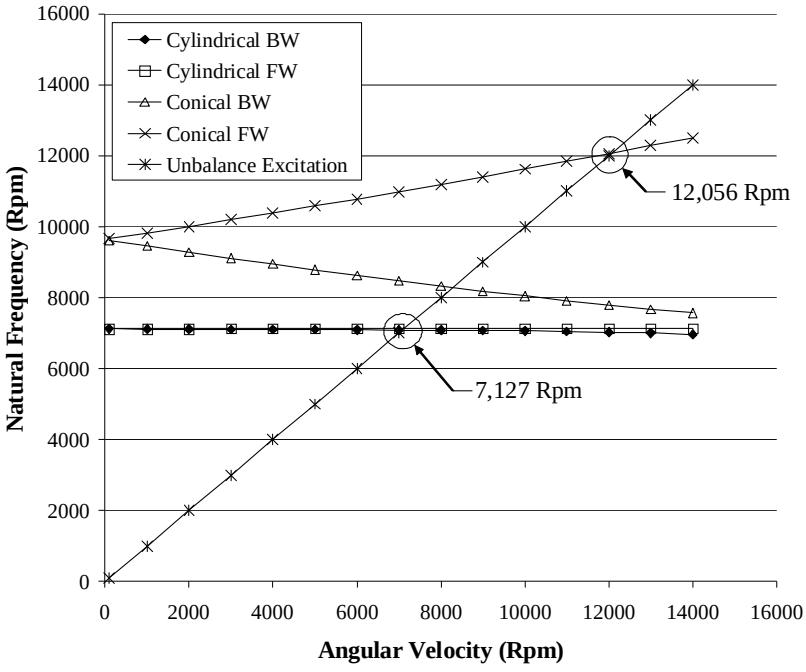

Figure 9 Predicted Campbell Diagram for Cylindrical and Conical Modes

Dr. Alan Palazzolo, a-palazzolo@tamu.edu, Texas A&M University, Mechanical Engineering, College Station, Tx., 77843-3123, 979-845-5280

(4) Components and Component Testing

Position sensing of the shaft was made utilizing Bently Nevada eddy cuuren, proximity probes with a bandwidth of approximately 5 khz and DC gain of approximately 200 mv/mil, wher 1 mil = 0.001 inches. The ultimate objective of the project was to develop FESS for satellite battery replacements or for combined attitude control and energy storage (ACESE) [5, 6]. These applications require electronics that are radiation hardened. A digital controller approach utilizing FPGA's or DSP would cost several hundred thousand dollars and require extensive lead times. Thus it was decided to build the analog suspension controller from analog components that had more readily available rad-hardened counterparts. Figure 10 shows an analog controller for flywheel magnetic suspension. The radial path transfer function is also show in Figure 10. The PD, notch and filter stage effects are clearly shown.

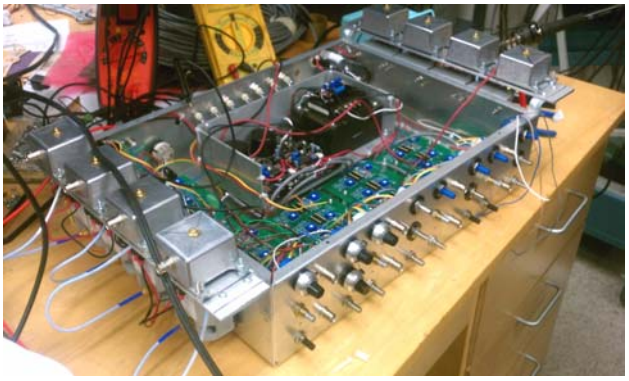

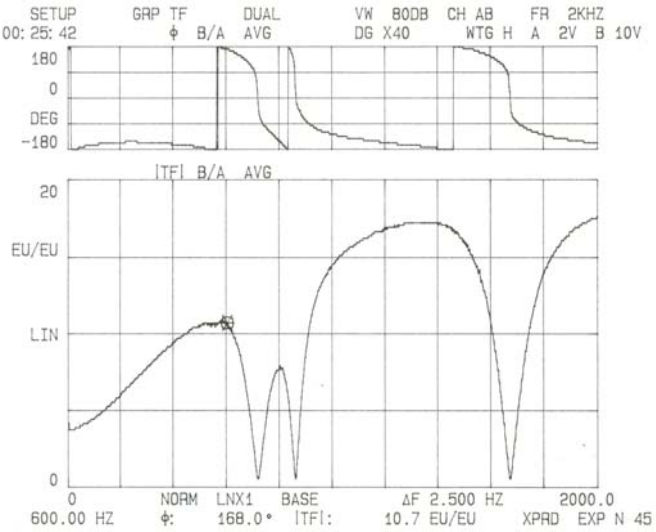

Figure 10 Five (5) Axis Magnetic Bearing Controller and Radial Path Transfer Function

Figure 11 Radial, Homopolar Magnetic Bearing and Rotating Assembly

Figure 11 shows the radial magnetic bearing actuator in its fully potted state. Loads were applied to the shaft and deflections were measured to determine the voltage and position stiffnesses and load capacities of the radial and combination bearings, where the linearized force representation of the actuator is given by:

$$F = k_v v + k_{pos} x \qquad (1)$$

Dr. Alan Palazzolo, a-palazzolo@tamu.edu, Texas A&M University, Mechanical Engineering, College Station, Tx., 77843-3123, 979-845-5280

and k_v and k_{pos} are the voltage and position stiffness, respectively. Figure 12 shows a photo of the setup and a position stiffness vs. journal position plot. Inductances were also measured in addition to the force characteristics. Table 1 summarizes the measured and predicted values for the radial and combo bearing.

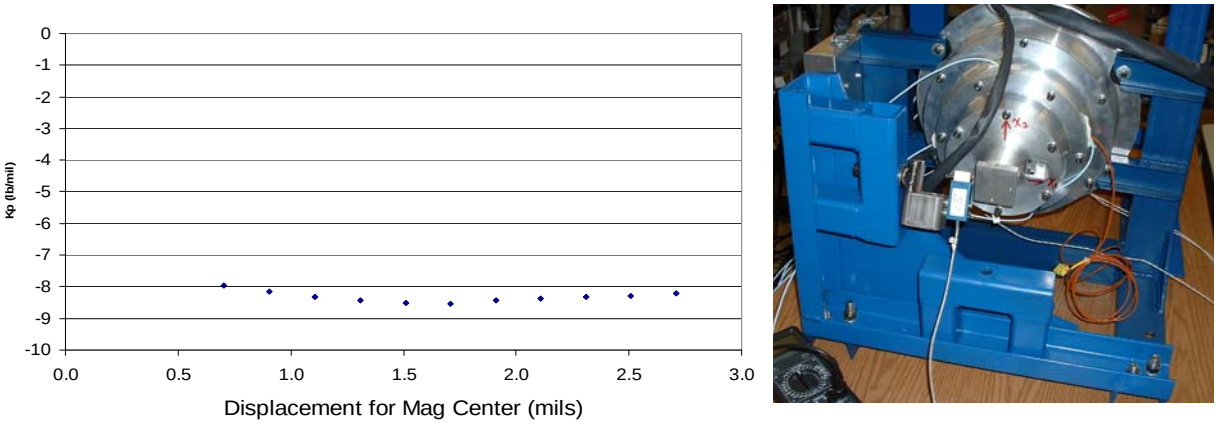

Figure 12 Measured Position Stiffness in lbs/mil and Test Fixture

G2 Radial Bearing Parameters				
	Predicted Value		Measured Value	
Position Stiffness	-6.16	*lbs/mil*	-6.8	*lbs/mil*
Current Stiffness	8.8	*lbs/Amp*	10.4	*lbs/Amp*
Load Capacity	70	*lbs*	85	*lbs*
Bias Flux Density	---	*Tesla*	0.82	*Tesla*
Pole Inductance	1.35	*mH*	1.2	*mH*

G2 Combo Bearing Parameters				
	Predicted Value		Measured Value	
Position Stiffness	-6.9	*lbs/mil*	-8.3	*lbs/mil*
Current Stiffness	9.3	*lbs/Amp*	8.5	*lbs/Amp*
Load Capacity	74	*lbs*	90	*lbs*
Bias Flux Density	0.82	*Tesla*	---	*Tesla*
Pole Inductance	1.35	*mH*	---	*mH*

Table 1. The current stiffnesses shown are determined using the currents in certain reference poles on the bearings since there exists 6 currents per bearing. The corresponding voltage stiffnesses were: 13.5 lbs/V for the radial bearing and 12. lbs/V for the combination bearing, where the voltage is the controller output voltage

Dr. Alan Palazzolo, a-palazzolo@tamu.edu, Texas A&M University, Mechanical Engineering, College Station, Tx., 77843-3123, 979-845-5280

The rotor was intentionally levitated with the journal positioned in a 4 mil offset eccentric position. The measured radial bearing, bias flux densities for this position are indicated in Figure 13. The inductance was measured in each of the 6 poles of the radial bearing with the journal shimmed to its centered position as shown in Figure 14 . The L values are shown in Table 2.

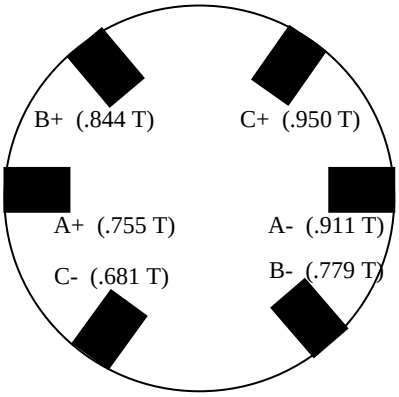

Figure 13 Measured Bias Flux Densities in Offset Radial Bearing

Figure 14 Radial Bearing Centered for Inductance Measurement

Bearing Pole	Inductance (mH)
A+	1.054
B+	1.114
C+	1.327
A-	1.253
B-	1.136
C-	1.161
Average	**1.174**

Predicted	**1.35**

Table 2 Measured Radial Bearing L's

(5) FLIGHT HARDWARE AND TEST DATA

The FESS was successfully tested in a vacuum spin pit in the author's lab at Texas A&M as shown in Figure 15(a). The unit was then transferred to a custom vacuum, containment vessel and installed on the airplane as shown in Figure 15(b). Vacuum pumps, recorders, UPS units, and the power and control electronics were mounted on a rack for the flight as shown in Figure 15(c, d).

(a)

(b)

(c)

(d

Figure 15 (a) Spin Pit Test at Texas A&M, (b) Vacuum Vessel on C-9, (c, d) Instrument Rack

The NASA C-9 flew departed from Ellington Field near Galveston Bay in Texas and flew approximately 100 zero "g" parabolas flying E-W across the Gulf of Mexico. Co-authors Johnson, Thomas and Little are shown operating the FESS and capturing data in Figure 16. The parabolic flight profile provided 15 - 20 seconds of micro-g conditions per parabola, 45 seconds of 1.8 g conditions between parabolas. The flywheel's spin axis was directed along the wing to wing (Y) direction. The Z direction is vertical as sensed by a passenger on the plane, and the X direction is front to rear as sensed on the plane. Four flight series were performed with 40 parabolas per series. The series objectives were:

Figure 16 FESS Operation on the C-9

Dr. Alan Palazzolo, a-palazzolo@tamu.edu, Texas A&M University, Mechanical Engineering, College Station, Tx., 77843-3123, 979-845-5280

First flight series — constant speed during parabolas (all speed changes made during level (1-g) flight)
Second flight series — constant acceleration during parabolas (all speed changes made during 0–g/2–g parabolas)
Third flight series — energy transfer during parabolas
Fourth flight series — start-up, impulse test and high-g test
Stable control of the flywheel was maintained under all conditions during all flights. Sample test results are provided in the following figures.

(a)

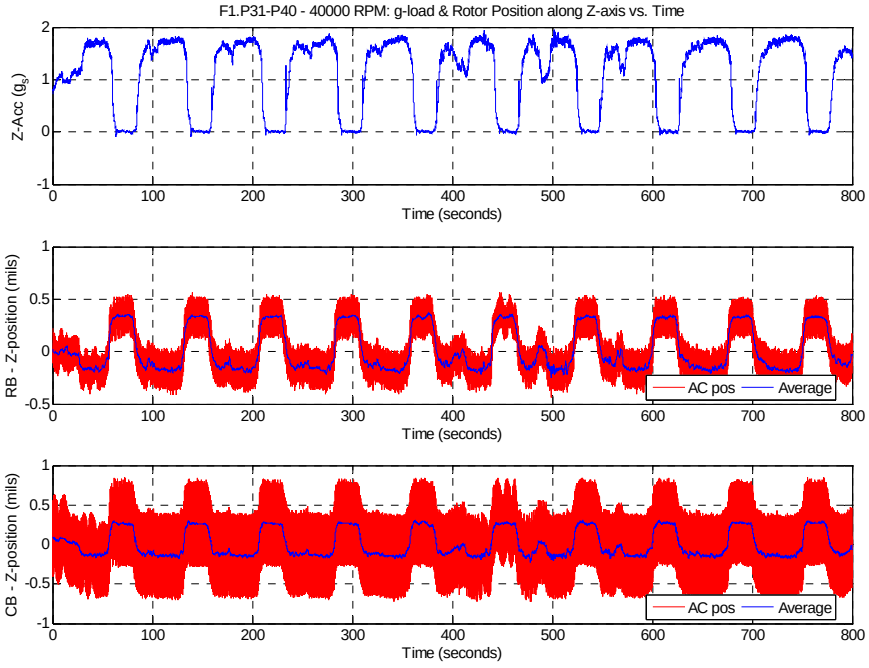

(b)

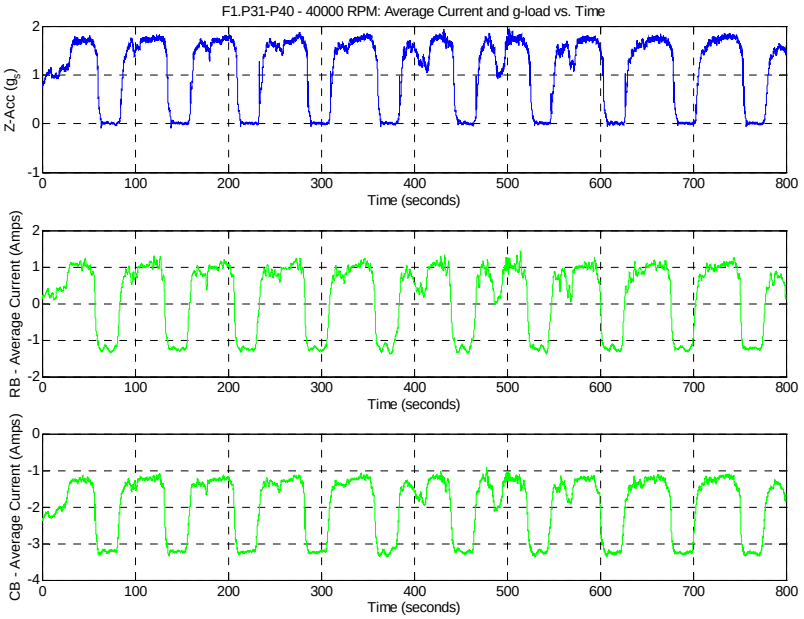

Figure 17 (a) Plane Acceleration, Journal Motions (mils) and (b) Bearing Currents (amps) in Parabolas at 40,000 rpm

Dr. Alan Palazzolo, a-palazzolo@tamu.edu, Texas A&M University, Mechanical Engineering, College Station, Tx., 77843-3123, 979-845-5280

Figure 17(a) shows the Z direction acceleration of the plane (top trace) and the Z direction relative motion of the journals in the magnetic bearings during 11 consecutive parabolas with the flywheel speed held constant at 40,000 rpm. The total motions (red) and running average motions (blue) are less than approximately $\pm 0.5 mils$, which is an insignificant deflection relative to the radial $20\ mil$ magnetic bearing clearance or radial $5\ mil$ catcher bearing clearance. Figure 17 (b) shows some currents in the magnetic bearings during this flight sequence. Figure 18 shows sample journal orbits at 39,000 rpm.

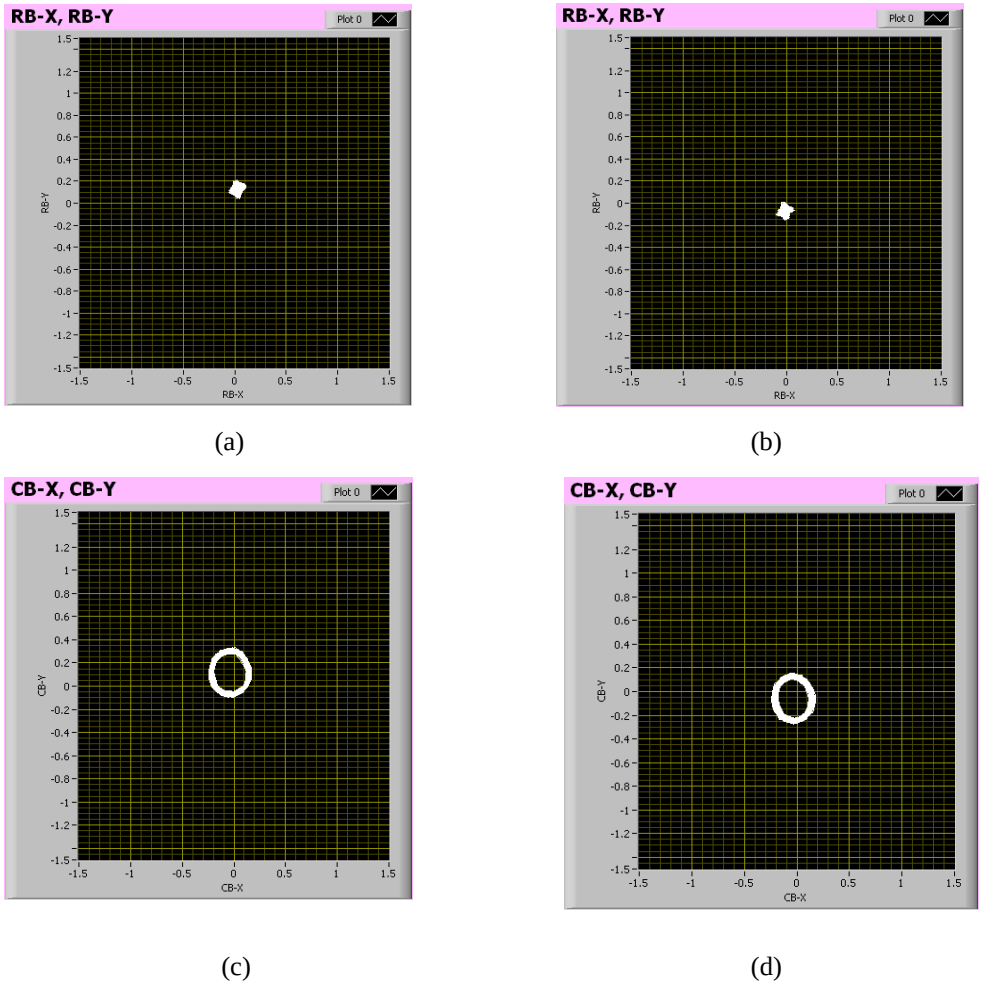

Figure 18 Journal Orbits with DC Shifts at 39,000 rpm for (a) Radial Bearing – 0 g, (b) Radial Bearing -2 g, (c) Combo Bearing – 0 g, (d) Combo Bearing -2 g,

Figure 19 shows speed, stored energy and power of the FESS during controlled acceleration tests over 10 consecutive parabolas. No significant deviations in vibration or journal motion from those shown in Figures 17 and 18 were detected. Figure 20 shows the "g" loading and journal Z motions during a sustained 2 g loading maneuver.

Dr. Alan Palazzolo, a-palazzolo@tamu.edu, Texas A&M University, Mechanical Engineering, College Station, Tx., 77843-3123, 979-845-5280

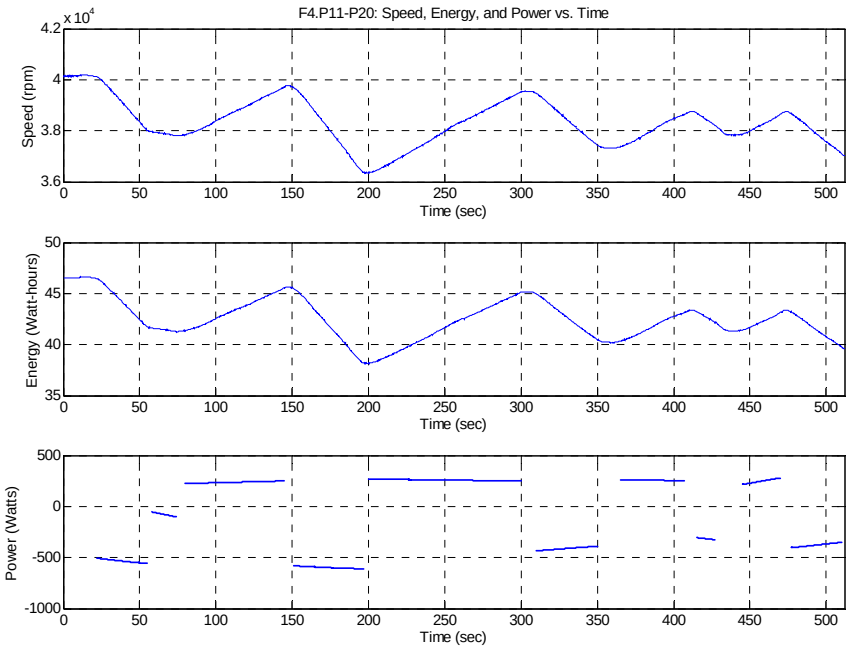

Figure 19 Speed, Energy and Power During Controlled Acceleration Tests Over 10 Parabolas

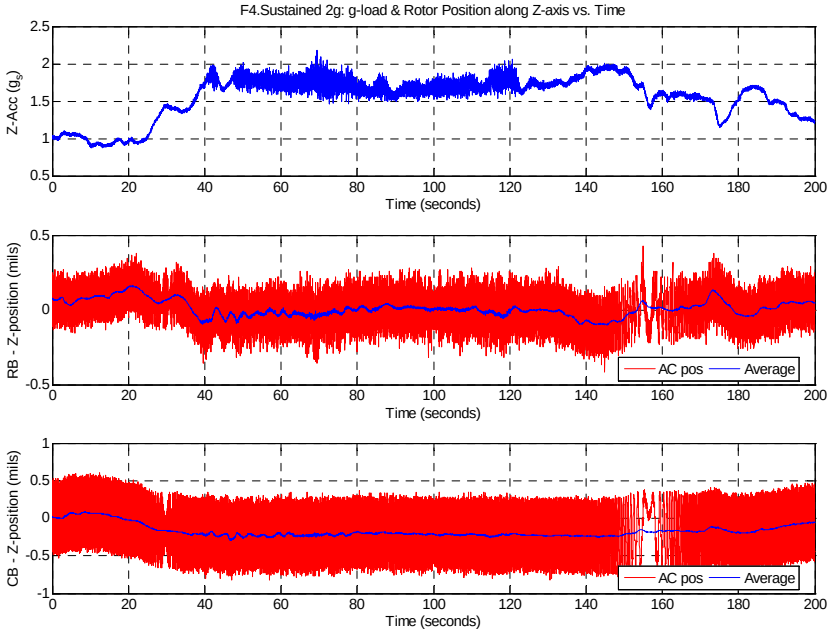

Figure 20 Plane g Loading and Journal Motions During a sustained 2 g Maneuver

Dr. Alan Palazzolo, a-palazzolo@tamu.edu, Texas A&M University, Mechanical Engineering, College Station, Tx., 77843-3123, 979-845-5280

(6) SUMMARY

Summary: The objective of successfully demonstrating levitation of a low energy flywheel under zero g conditions was successfully met. The predicted component and system response characteristics showed good agreement. Relative journal displacements did not exceed approximately 0.5 mils peak over all the tests. These motions were small enough to lower the catcher bearing clearances to approximately 0.004" radial. The control employed was PD with lead, lag, and notch filter stages.

A high frequency instability occurred during the controller tuning phase. The resulting response was a limit cycle of an approximate 0.003" peak – peak amplitude near 700 hz. This type of response had been previously observed commissioning another flywheel and was casually referred to as a "virtual catcher bearing" since although a large motion occurred the shaft never contacted the catcher bearing. We recently found the explanation for this in the effects of current saturation (limiting) in the servo power amplifier as depicted in figure 21.

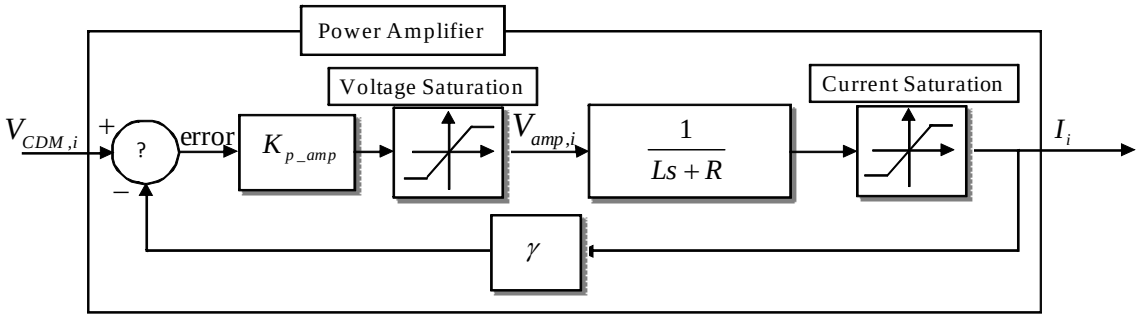

Fig. 21 Simplified power amplifier model with output voltage and current saturation limiters

This effect may also be caused by flux saturation. The interested reader may find a comprehensive discussion of this in reference [7].

Future work in this area includes testing higher energy, higher gyroscopic (Ip/It) flywheels under similar conditions. In addition similar flight tests of combined attitude control and energy storage systems is likewise recommended.

(7) ACKNOWLEDGEMENTS

The authors gratefully acknowledge the technical contribution of Dr. Andrew Kenny, formerly of Texas A&M University, and the guidance of Mr. Raymond Beach of NASA Glenn and Mr. Fred Best, formerly of the Texas A&M Center for Space Power. We thank NASA and the Texas A&M Center for Space Power for funding this effort.

(8) REFERENCES

[1] Palazzolo, A.B., et. al. "Fault Tolerant Homopolar Magnetic Bearings", *U.S. Patent 7,429,811*

[2] Li, Ming Hsiu, Palazzolo,A., Kenny, A., Provenza, A., Beach,R., Kascak,A., "Fault Tolerant Homopolar Magnetic Bearings", *IEEE Trans. On Magnetics*, Vol. 40, No. 5, Sept. 2004, pp. 3308 – 3318.

[3] Maslen, E, and Meeker, D., Fault Tolerance of Magnetic Bearings by Generalized Bias Current

Dr. Alan Palazzolo, a-palazzolo@tamu.edu, Texas A&M University, Mechanical Engineering, College Station, Tx., 77843-3123, 979-845-5280

Linearization, *IEEE Trans. On Magnetics*, 1995

[4] Palazzolo, A., Mu Li, Uhn Joo Na, Erwin Thomas, "System and Method for Controlling Suspension Using a Magnetic Field", ***US Patent: (US 6,323,614B1)***; Date of Patent: Nov. 27, 2001; Inventors:

[5] Park, J., Palazzolo, A. and Beach, R., " MIMO Active Vibration Control of Magnetically Suspended Flywheels for Satellite IPAC Service", *ASME J. Dynamic Systems Measurements and Controls*, Vol. 130 July 2008.

[6] Park, J. and Palazzolo, A., Magnetically Suspended VSCMGs for Simultaneous Attitude Control and Power Transfer IPAC Service, *ASME J. Dyn. Sys., Meas., Control* , September 2010, Volume 132, Issue 5, 051001 (15 pages)

[7] Kang, Kyung-dae and Palazzolo, A. Homopolar Magnetic Bearing Saturation Effects on Rotating Machinery Vibrations, *IEEE Trans. On Magnetics*, Vol. 48 , Issue 6, pp. 1984-1994, June 2012.

Dr. Alan Palazzolo, a-palazzolo@tamu.edu, Texas A&M University, Mechanical Engineering, College Station, Tx., 77843-3123, 979-845-5280